第 35 卷第 9 期
2019 年 9 月

无 机 化 学 学 报
CHINESE JOURNAL OF INORGANIC CHEMISTRY

Vol.35 No.9
1570-1578

氰基桥联的 Fe_2Ni 双之字链的合成与磁性

贺艳丽　孟银杉　孙慧莹　姜文静　矫成奇　刘　涛*
(大连理工大学精细化工国家重点实验室,大连　116024)

摘要：利用四氰基构筑单元和不同位阻的吡啶类配体,合成了 3 例氰基桥联的 $Fe^{Ⅲ}_2Ni^{Ⅱ}$ 链状化合物。化合物{[Fe(bpy)$(CN)_4]_2$[Ni$(bp)_2]\cdot 2H_2O\}_n$ (**1**)(bpy=2,2′-联吡啶;bp=4-苯基吡啶),{[Fe(bpy)$(CN)_4]_2$[Ni$(papy)_2]\cdot H_2O\}_n$ (**2**)(papy=4-(苯基氮烯)吡啶)和{[Fe(bpy)$(CN)_4]_2$[Ni$(azp)]\cdot 4H_2O\}_n$ (**3**)(azp=1,2-二(吡啶-4-基)二氮烯)均为双之字型的链状结构。磁性测试表明化合物 **1**~**3** 均表现为链内的铁磁相互作用。化合物 **1** 表现出单链磁体行为,有效能垒为 10.9 K。

关键词：氰基桥联；双之字链；铁磁性；单链磁体。
中图分类号：O614.81+1；O614.81+3　　**文献标识码**：A　　**文章编号**：1001-4861(2019)09-1570-09
DOI:10.11862/CJIC.2019.176

Synthesis and Magnetism of Cyano-Bridged Fe_2Ni Double-Zigzag Chains

HE Yan-Li　MENG Yin-Shan　SUN Hui-Ying　JIANG Wen-Jing　JIAO Cheng-Qi　LIU Tao*
(*State Key Laboratory of Fine Chemicals, Dalian University of Technology, Dalian, Liaoning* 116024, *China*)

Abstract: Three cyano-bridged Fe_2Ni chain compounds were synthesized via the reaction of tetracyanometallate building block and pyridine ligands with different steric hindrance. Compounds {[Fe(bpy)$(CN)_4]_2$[Ni$(bp)_2]\cdot 2H_2O\}_n$ (**1**) (bpy=2,2′-bipyridine; bp=4-phenylpyridine), {[Fe(bpy)$(CN)_4]_2$[Ni$(papy)_2]\cdot H_2O\}_n$ (**2**) (papy=4-(phenyldiazenyl) pyridine) and {[Fe(bpy)$(CN)_4]_2$[Ni(azp)]$\cdot 4H_2O\}_n$ (**3**) (azp=1,2-di(pyridin-4-yl)diazene) all show double-zigzag chain-like structures. Magnetic study indicates that compounds **1**~**3** all show intrachain ferromagnetic interactions. Alternating current susceptibility measurements demonstrated the single-chain magnet behavior of compound **1** with the relaxation energy barrier E_a/k_B of 10.9 K. CCDC: 1904149, **1**; 1904150, **2**; 1904151, **3**.

Keywords: cyano-bridged; double-zigzag chain; ferromagnetic; single-chain magnets

0 Introduction

Single-chain magnets (SCMs), which can exhibit slow magnetic relaxation and magnetic hysteresis below blocking temperature, have attracted considerable attention and great interests because of their potential application in high-density information storage and spintronic devices[1-8]. This conception was firstly proposed by Glauber in 1960s that Ising magnetic chain was expected to exhibits low magnetic relaxation behavior[9]. However, it was not until 2001 Gatteschi and co-workers reported the first single-chain magnet [Co$(hfac)_2$(NITPHOMe)][10]. In recent decades, considerable SCMs with chirality, porosity, spin-crossover, photo-switchable properties have been reported[10-16]. In order to obtain high-performance SCMs, two challenges have to be solved: (1) constructing magnetic chains with strong intrachain ferromagnetic interactions so as to meet the Ising chain requirement; (2) minimizing the interchain interaction to avoid the long-range

收稿日期:2019-03-20。收修改稿日期:2019-06-30。
国家自然科学基金(No.21871039,21801037)资助项目。
*通信联系人。E-mail:liutao@dlut.edu.cn

magnetic ordering. Utilizing metallocyanate building blocks as multidentate ligands is an effective approach for constructing SCMs for that it is helpful to form the one-dimensional structure and transmit the intrachain magnetic interactions[14,17-19]. Particularly, tetracyanometallate building block facilitates the construction of one-dimensional chain structure, wherein two of the four cyano groups can coordinate with appropriate metal ions to form a double-zigzag chain, and the other two cyano groups can form hydrogen bonding interactions with solvent molecules. The recent study have also dedicated the important role of tetracyanometallate building blocks in the construction of photo-switchable single-chain magnets[20-21].

In order to obtain the SCMs, we plan to use tetracyanometallate building block to link spin carriers such as Co^{2+}, Ni^{2+}, Mn^{3+} and Fe^{2+} into a ferromagnetic chain. The interchain magnetic interaction should be minimized to avoid the long-range ordering. Therefore, suitable diamagnetic auxiliary ligands should be carefully selected to make chains magnetically well-isolated and ensure the uniaxial anisotropy of the transition metal ions[11,13,22-25]. In this work, we selected Li[Fe(Ⅲ)(bpy)$(CN)_4$] (bpy=2,2′-bipyridine) as the building block to react with Ni(Ⅱ) ions. The Ni(Ⅱ) ion was chosen because the interactions between low-spin Fe(Ⅲ) and high-spin Ni(Ⅱ) are generally ferromagnetic. Three auxiliary ligands 4-phenylpyridine (bp), 4-(phenyldiazenyl)pyridine (papy), and 1,2-di(pyridin-4-yl)diazene (azp) were applied, forming three cyano-bridged $Fe^{Ⅲ}_2Ni^{Ⅱ}$ double-zigzag chain complexes: {[Fe(bpy)$(CN)_4]_2$[Ni(bp)$_2$]·$2H_2O$}$_n$ (**1**), {[Fe(bpy)$(CN)_4]_2$[Ni(papy)$_2$]·H_2O}$_n$ (**2**) and {[Fe(bpy)$(CN)_4]_2$[Ni(azp)]·$4H_2O$}$_n$ (**3**). Herein, we reported the synthesis, crystal structures and magnetic properties of compounds **1**~**3**.

1 Experimental

1.1 Materials and methods

All organic reagents were commercially obtained and used without further purification. Li[Fe(bpy)$(CN)_4$] and the ancillary ligands L (L=bp, papy and azp) were synthesized according to the literature methods[26]. Elemental analyses (C, H and N) were performed on an ElementarVario EL Ⅲ analyzer. Magnetic measurements of the samples were performed on a Quantum Design SQUID (MPMS XL-7) magnetometer. Data were corrected for the diamagnetic contribution calculated from Pascal constants.

1.2 Synthesis of {[Fe(bpy)$(CN)_4]_2$[Ni(bp)$_2$]·$2H_2O$}$_n$ (1)

A 1.0 mL aqueous solution of Ni$(BF_4)_2$·$6H_2O$ (0.005 mmol) was placed at the bottom of a test tube, a mixture of methanol and water (1:4, *V*/*V*, 2 mL) was gently layered on the top of the solution, and then a 1.0 mL methanol solution of Li[Fe(bpy)$(CN)_4$] (0.01 mmol) and 4-phenylpyridine (0.01 mmol) was carefully added as the third layer. After four weeks, red crystals of **1** were obtained and collected after washed with water and air dried. Yield: 57% based on Ni$(BF_4)_2$·$6H_2O$. Anal. Calcd. for $C_{50}H_{38}Fe_2N_{14}NiO_2$(%): C 57.84, H 3.66, N 18.89; Found(%): C 57.76, H 3.62, N 18.72.

1.3 Synthesis of {[Fe(bpy)$(CN)_4]_2$[Ni(papy)$_2$]·H_2O}$_n$ (2)

Red crystals of compound **2** were obtained and collected in the same way as for compound **1**, except using 4-(phenyldiazenyl)pyridine (0.01 mmol) to replace 4-phenylpyridine (0.01 mmol). Red crystals appeared after four weeks. Yield: 61% based on Ni$(BF_4)_2$·$6H_2O$. Anal. Calcd. for $C_{50}H_{36}Fe_2N_{18}NiO$(%): C 55.79, H 3.35, N 23.43; Found(%): C 55.68, H 3.40, N 23.39.

1.4 Synthesis of {[Fe(bpy)$(CN)_4]_2$[Ni(azp)]·$4H_2O$}$_n$ (3)

One milliliter aqueous solution of Ni$(ClO_4)_2$·$6H_2O$ (0.005 mmol) was placed at the bottom of a test tube. A mixture of methanol and water (1:2, *V*/*V*, 2 mL) was gently layered on the top of the solution, and then 1.0 mL methanol solution of Li[Fe(bpy)$(CN)_4$] (0.01 mmol) and 1,2-di(pyridin-4-yl)diazene (0.01 mmol) was carefully added as the third layer. After few weeks, red crystals of **3** were obtained and collected after washed with water and air dried. Yield: 54% based on Ni$(ClO_4)_2$·$6H_2O$. Anal. Calcd. for $C_{38}H_{32}Fe_2N_{16}NiO_4$(%): C 48.14, H 3.38, N 23.65; Found(%): C 48.20, H 3.32, N 23.58.

1.5 X-ray crystallography

The data were collected on a Bruker Smart APEX Ⅱ X-diffractometer equipped with graphite

monochromated Mo $K\alpha$ radiation (λ=0.071 073 nm) using the SMART and SAINT[27] programs at 298 K for compounds **1~3**. Final unit cell parameters were based on all observed reflections from integration of all frame data. The structures were solved in the space group by direct method and refined by the full-matrix least-squares using SHELXTL-97 fitting on F^2 [28]. For compounds **1~3**, all non-hydrogen atoms were refined anisotropically. The hydrogen atoms of organic ligands were located geometrically and fixed isotropic thermal parameters. The crystal data and details of the structure refinement of compounds **1 ~3** are summarized in Table 1. Selected bond distances and angles of compounds **1~3** are listed in Table 2.

CCDC: 1904149, **1**; 1904150, **2**; 1904151, **3**.

Table 1 Crystal data and structure refinements for compounds 1~3

Compound	1	2	3
Formula	$C_{50}H_{38}Fe_2N_{14}NiO_2$	$C_{50}H_{36}Fe_2N_{18}NiO$	$C_{38}H_{32}Fe_2N_{16}NiO_4$
Formula weight	1 037.35	1 075.38	947.20
Crystal system	Monoclinic	Triclinic	Monoclinic
Space group	*C*2/*c*	$P\bar{1}$	*I*2/*m*
a / nm	2.746 9(4)	0.646 13(3)	0.662 18(5)
b / nm	1.531 4(3)	1.387 02(7)	2.824 22(19)
c / nm	1.346 4(2)	1.481 53(7)	1.247 16(8)
α / (°)		109.834 0(10)	
β / (°)	115.369(3)	100.734 0(10)	98.491(4)
γ / (°)		101.992 0(10)	
V / nm^3	5.117 6(14)	1.173 2(10)	2.306 8(3)
Z	4	1	2
D_c / (g·cm^{-3})	1.346	1.522	1.364
F(000)	2 128	550	968
Reflection collected	15 884	43 991	21 420
Unique reflection (R_{int})	4 510 (0.118 7)	4 099 (0.026 8)	2 705 (0.044 7)
Goodness-of-fit on F^2	0.940	1.067	1.224
R_1[a] [$I>2\sigma(I)$]	0.080 4	0.025 6	0.063 2
wR_2[b] [$I>2\sigma(I)$]	0.198 8	0.069 5	0.183 5

[a] $R_1=\sum(|F_o|-|F_c|)/\sum|F_o|$; [b] $wR_2=[\sum w(|F_o|-|F_c|)^2/\sum wF_o^2]^{1/2}$.

Table 2 Selected bond lengths (nm) and angles (°) for compounds 1~3

		1			
Fe(1)-C(12)	0.188 8(7)	Fe(1)-N(2)	0.196 8(5)	Ni(1)-N(4)	0.203 7(6)
Fe(1)-C(13)	0.189 1(7)	Fe(1)-N(1)	0.197 5(5)	Ni(1)-N(7)	0.210 1(7)
Fe(1)-C(11)	0.193 1(10)	Ni(1)-N(4)#1	0.203 7(6)	Ni(1)-N(5)#2	0.205 3(6)
Fe(1)-C(14)	0.195 3(10)	Ni(1)-N(5)#3	0.205 3(6)	Ni(1)-N(7)#1	0.210 1(7)
N(3)-C(11)-Fe(1)	178.7(7)	N(5)-C(13)-Fe(1)	179.1(7)	C(12)-N(4)-Ni(1)	170.1(6)
N(4)-C(12)-Fe(1)	174.9(7)	N(6)-C(14)-Fe(1)	176.9(8)	C(13)-N(5)-Ni(1)#3	161.4(5)
		2			
Fe(1)-C(12)	0.190 9(19)	Fe(1)-N(1)	0.197 7(15)	Ni(1)-N(4)#1	0.209 8(15)
Fe(1)-C(13)	0.191 1(19)	Fe(1)-N(2)	0.197 9(15)	Ni(1)-N(4)#2	0.209 8(15)
Fe(1)-C(14)	0.195 5(2)	Ni(1)-N(5)	0.212 2(16)	Ni(1)-N(5)#3	0.212 2(16)
Fe(1)-C(11)	0.196 4(2)	Ni(1)-N(7)	0.214 6(15)	Ni(1)-N(7)#3	0.214 6(15)

Continued Table 2

N(3)-C(11)-Fe(1)	177.46(17)	N(5)-C(13)-Fe(1)	173.68(16)	C(13)-N(5)-Ni(1)	149.08(14)
N(4)-C(12)-Fe(1)	172.19(16)	N(6)-C(14)-Fe(1)	178.11(18)	C(12)-N(4)-Ni(1)#4	163.85(14)
		3			
Fe(1)-C(7)	0.191 4(4)	Fe(1)-N(1)#4	0.197 7(4)	Ni(1)-N(3)#2	0.207 6(4)
Fe(1)-C(7)#4	0.191 1(4)	Fe(1)-N(1)	0.197 7(4)	Ni(1)-N(3)#3	0.207 6(4)
Fe(1)-C(6)#4	0.191 4(4)	Ni(1)-N(3)	0.207 7(4)	Ni(1)-N(5)#1	0.210 5(5)
Fe(1)-C(6)	0.194 6(5)	Ni(1)-N(3)#1	0.207 6(4)	Ni(1)-N(5)	0.210 5(5)
N(2)-C(6)-Fe(1)	178.1(5)	N(3)-C(7)-Fe(1)	172.3(4)	C(7)-N(3)-Ni(1)	160.7(4)

Symmetry transformations used to generate equivalent atoms: #1: $-x+2, -y+1, -z+2$; #2: $x, -y+1, z+1/2$; #3: $x+2, y, -z+3/2$ for **1**; #1: $-x+1, -y+1, -z+1$; #2: $x-1, y, z$; #3: $-x, -y+1, -z+1$; #4: $x+1, y, z$ for **2**; #1: $-x, -y, -z$; #2: $x, -y, z$; #3: $-x, y, -z$; #4: $-x+1, y, -z$ for **3**.

2　Results and discussion

2.1　Structure characterization

Single-crystal X-ray diffraction analysis revealed that **1** crystallizes in the monoclinic space group $C2/c$, **2** in the triclinic space group $P\bar{1}$, and **3** in the monoclinic space group $I2/m$, respectively (Table 1). All of them show a similar skeleton, constructed by the cyano-bridged $Fe^{Ⅲ}_2Ni^{Ⅱ}$ double-zigzag chains. Uncoordinated water molecules are located between the chains. Each repeating unit comprises of neutral $[Fe(bpy)(CN)_4]_2Ni(L)_2$, in which each nickel ion is coordinated with two ligands L along the apical direction. Different from compounds **1** and **2**, the neutral layer of compound **3** is further linked by the bidentate ligands along the apical direction of the Ni(Ⅱ) centers. Within the repeating unit, the nickel ion is coordinated by two nitrogen atoms from the ligands L and four cyanide nitrogen atoms from two contiguous $[Fe(bpy)(CN)_4]^-$ portions. Each iron ion is located in an octahedral environment, comprising four carbon atoms from the cyanide groups and two nitrogen atoms from the bidentate ligand bpy.

For compound **1**, the Fe-N and Fe-C bond lengths are 0.197(5)~0.198(5) nm and 0.189(7)~0.195(10) nm, respectively, which are characteristic of the LS Fe(Ⅲ) ions. The Ni-N bond distances are in a range of 0.204(6)~0.210(7) nm, which are in good agreement with those of high-spin Ni(Ⅱ) compounds. The Fe-C≡N angles are almost linear with bond angles of 174.9(7)°~179.1(7)°. The values of the C≡N-Ni angles are 161.4(5)°~170.1(6)°. Meanwhile, the $\pi\cdots\pi$ (0.376 1 nm) stacking interactions exist between the pyridine rings of adjacent bpy ligands and aromatic rings of the

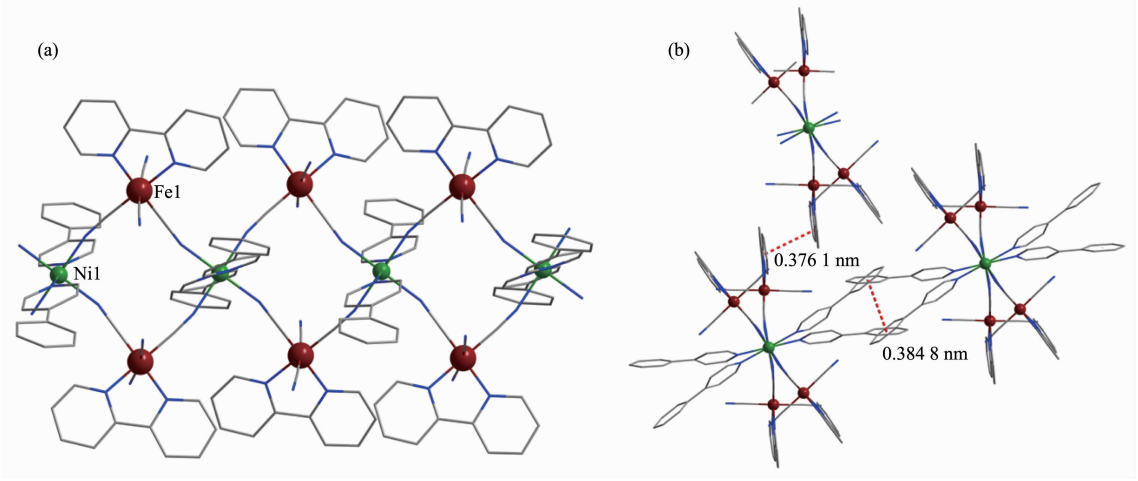

H atoms have been omitted for clarity; Atomic scheme: Fe, red; Ni, green; C, grey; N, blue

Fig.1　(a) Side view of 1D double-zigzag chain of **1**; (b) Packing structures of **1** via $\pi\cdots\pi$ stacking interactions

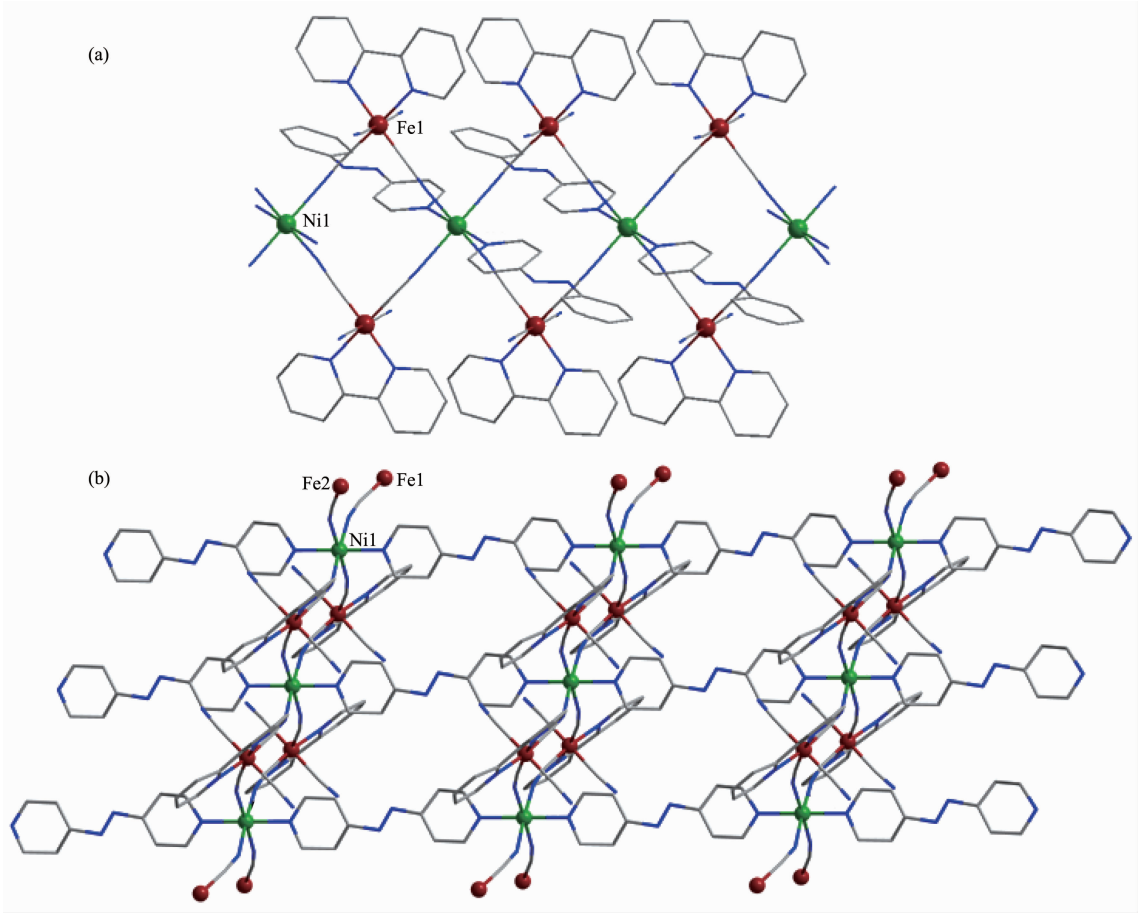

H atoms have been omitted for clarity; Atomic scheme: Fe, red; Ni, green; C, grey; N, blue

Fig.2 (a) Side view of a 1D double-zigzag chain of **2**; (b) Front view of a 3D double-zigzag chain of **3**

adjacent 4-phenylpyridine ligands. The nearest distance between the adjacent pyridine rings is 0.376 1(2) nm, and the nearest distance of aromatic rings of the 4-phenylpyridine ligands is 0.384 8 (2) nm. The shortest intrachain Fe…Fe, Fe…Ni and Ni…Ni distances are 0.707 8(3), 0.502 9(2) and 0.675 9(3) nm, respectively. The nearest interchain Ni…Ni distance is 1.454 8(6) nm, which indicates that interchain magnetic interactions should be weak.

For compound **2**, the Fe-N and Fe-C bond lengths are in a range of 0.197 7(15)~0.197 9(15) nm and 0.190 9(19)~0.196 4(2) nm, respectively. The Ni-N distances range from 0.209 8(15) to 0.214 6(15) nm. The Fe-C≡N linkages are close to linearity with bond angles of 172.2(16)°~178.1(18)°. The bond lengths and bond angles of compound **2** confirm that the Fe(Ⅲ) is in the low-spin state. In comparison with compound **1**, the C≡N-Ni angles fall in a range of 149.08(14)°~163.85(14)°, which depart significantly from linearity. The shortest intrachain Fe…Fe, Fe…Ni and Ni…Ni distances are 0.646 1(20), 0.507 0(34) and 0.646 1(47) nm, respectively. The nearest interchain Ni…Ni distance is 1.403 2(41) nm.

For compound **3**, the Fe-N (0.197 7(4) nm) and Fe-C (0.191 1(4)~0.194 6(5) nm) bond lengths are in good agreement with the reported LS Fe(Ⅲ) compounds. The Ni-N bond distances are 0.207 6(4)~0.210 5(5) nm. The Fe-C≡N angles deviate slightly from linearity, which are in a range of 172.3(4)°~178.1(5)°. The values of the C≡N-Ni angles are 160.7(4)°. The shortest intrachain Fe…Fe, Fe…Ni and Ni…Ni distances are 0.662 2(5), 0.500 9(7) and 0.662 2(5) nm, respectively. The nearest interchain Ni…Ni distance is 1.322 9(8) nm. Compared with compounds **2** and **3**, compound **1** exhibits longer interchain distances, which may diminish the interchain magnetic interactions and

benefit for slow magnetic relaxation of SCMs. To further elucidate the differences of them, we applied geometry analysis to see how the ancillary ligands influence the coordination environment of Ni(Ⅱ) ion (Table 3). One can note that coordination environments of Ni(Ⅱ) in compounds **1**~**3** are all octahedron type and the CShM value of Ni for compound **1** is the highest. This indicates that the Ni(Ⅱ) ion in **1** locates in a more distorted octahedron environment.

Table 3　SHAPE analysis of Ni six-coordinated geometry in compound 1~3

	HP-6 (D_{6h})	PPY-6 (C_{5v})	OC-6 (O_h)	TPR-6 (D_{3h})	JPPY-6 (C_{5v})
1	32.101	29.709	0.066	16.177	33.125
2	32.614	29.640	0.028	16.291	33.103
3	32.752	28.910	0.048	15.764	32.481

Abbreviation: HP: exagon, PPY: Pentagonal pyramid, OC: Octahedron, TPR: Trigonal prism, JPPY: Johnson pentagonal pyramid J2.

2.2　Magnetic characterizations

Temperature-dependent magnetic susceptibilities data of **1**~**3** were collected under a DC field of 1 000 Oe in a temperature range of 2~300 K (Fig.3). The χT

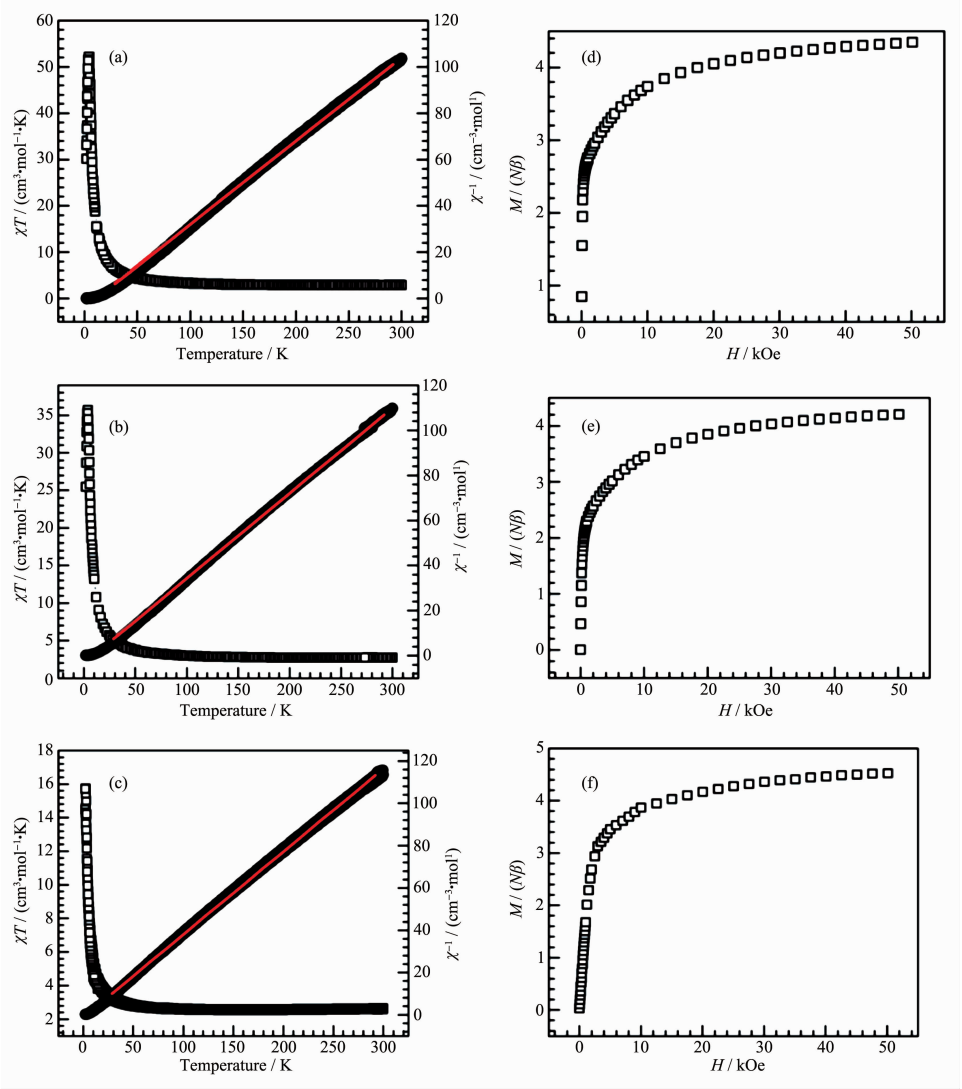

Solid line: the fitting to the Curie-Weiss law

Fig.3　Temperature-dependent magnetic susceptibilities of **1** (a), **2** (b) and **3** (c) in a temperature range of 2~300 K under an applied field of 1 000 Oe and field-dependent magnetizations of **1** (d), **2** (e) and **3** (f)

values for **1**, **2** and **3** were 2.90, 2.74 and 3.06 $cm^3 \cdot mol^{-1} \cdot K$ at 300 K, respectively, which are approximatively in a range of 2.48~2.80 $cm^3 \cdot mol^{-1} \cdot K$ expected for two LS Fe(Ⅲ) (S=1/2, g=2.6~2.8) and one HS Ni(Ⅱ) (S=1, g=2.2~2.3). When the temperature went down, χT values of **1**~**3** first increased smoothly and then increased rapidly at 80 , 60 and 50 K, respectively, reaching the maximum values of 52.16, 35.68 and 14.59 $cm^3 \cdot mol^{-1} \cdot K$ at 4.2, 3.9 and 2.4 K. The χT vs T plots indicate the typical ferromagnetic interaction between Fe(Ⅲ) and Ni(Ⅱ) ions within the chain. When the temperature decreased further to 2 K, the χT values of **1** and **2** decreased and reached the values of 33.1 and 25.50 $cm^3 \cdot mol^{-1} \cdot K$, respectively. It is probably caused by the zero-field splitting of Ni(Ⅱ) ions and/or weak interchain antiferromagnetic interactions. In the temperature range of 30~300 K, the magnetic susceptibility data of **1**~**3** were fitted with the Curie-Weiss law, giving Curie constant C of 2.78, 2.65 and 2.55 $cm^3 \cdot mol^{-1} \cdot K$ and Weiss constant θ of 11.27, 9.29 and 3.05 K, respectively. The positive Weiss constants of **1**~**3** further confirm the ferromagnetic coupling interactions between Fe(Ⅲ) and Ni(Ⅱ) ions. Meanwhile, the field-dependent magnetization at 2 K also confirms the ferromagnetic behavior. The isothermal magnetization of **1**~**3** first increased linearly and then increased gradually, reaching a maximum value of 4.35$N\beta$, 4.20$N\beta$ and 4.52$N\beta$ at 50 kOe, respectively. The values are close to the saturation value for two magnetically isolated low-spin Fe(Ⅲ) ions and one magnetically isolated high-spin Ni(Ⅱ) ion.

To further probe the dynamics of the magnetization of the three compounds, the alternating current (ac) magnetic susceptibilities were studied. For compounds **2** and **3**, no obvious frequency-dependent in-phase (χ') and out-of-phase signals (χ'') were observed, indicating that compounds **2** and **3** are not single-chain magnets (Fig.4(a) and (b)). For compound **1**, temperature- and frequency-dependent in-phase components (χ') were observed below 2.8 K, as shown

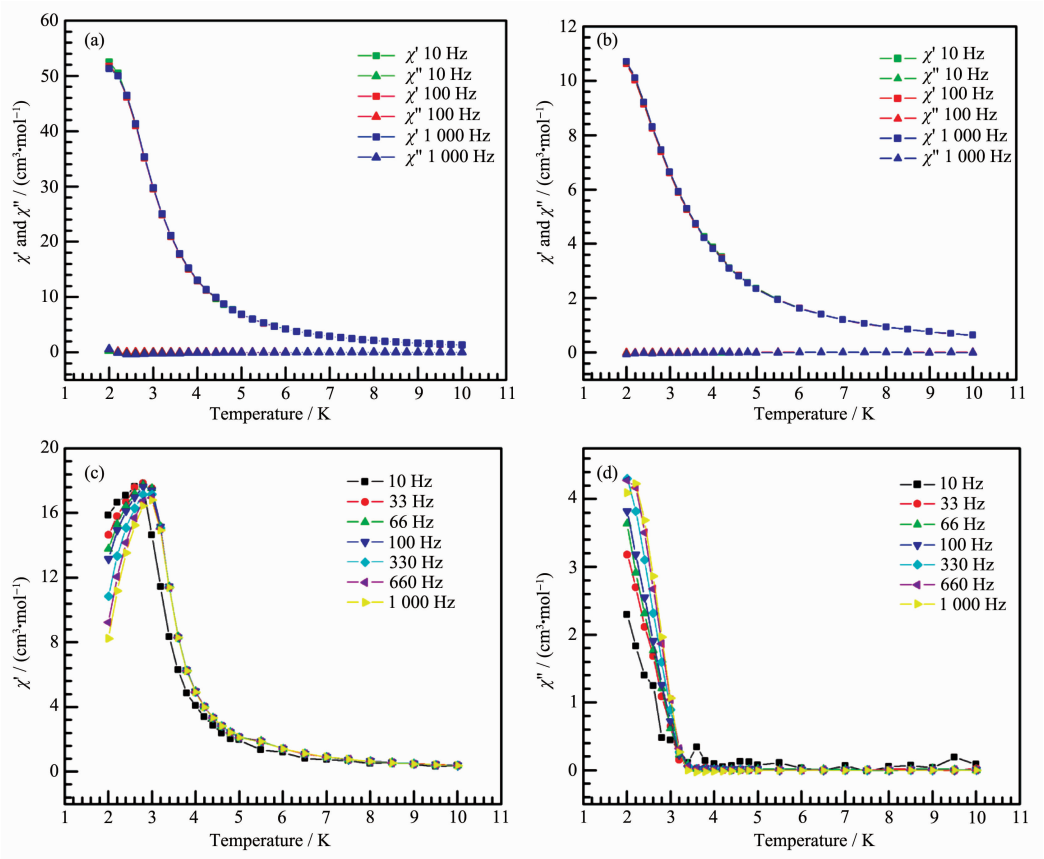

Fig.4 Frequency dependence of ac magnetic signals of compounds **2** (a) and **3** (b) at H_{ac}=3.5 Oe and H_{dc}=0 Oe; Frequency dependence of ac magnetic signals of compound **1** (c, d)

in Fig.4(c). Moreover, the plots of field-cooled magnetization (FC) and zero-field-cooled magnetization (ZFC) under a field of 100 Oe of **1** showed no bifurcation (Fig.5), excluding the spontaneous magnetization above 1.8 K. The generalized Debye model was used to extract the energy barrier based on the relationship of $\ln(\chi'/\chi'')=\ln(\omega\tau_0)+E_a/(k_BT)$. The obtained energy barrier E_a/k_B was 10.9 K and the relaxation time τ_0 was 7.8×10^{-4} s (Fig.6), which are in the typical range for SCMs.

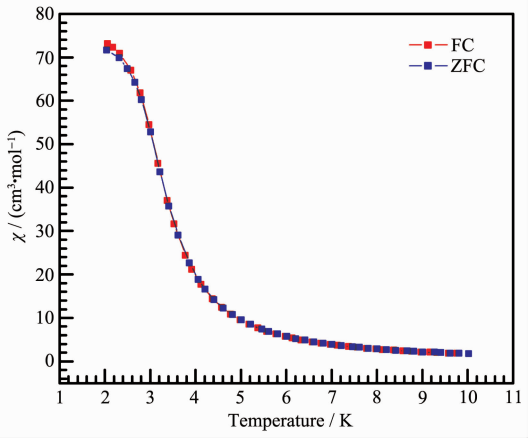

Fig.5　Field-cooled magnetization (FC) and zero field-cooled magnetization (ZFC) curves of compound **1**

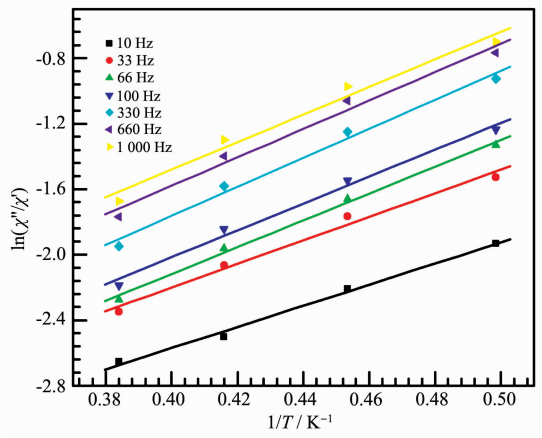

Solid line represents the fitting results over a range of 2.0~2.8 K

Fig.6　Plots of $\ln(\chi''/\chi')$ vs $1/T$ for **1**

Three cyano-bridged $Fe^{Ⅲ}_2Ni^{Ⅱ}$ double-zigzag chains show different magnetic behaviors. The neutral ancillary ligands should be the main reason for the different magnetic behaviors of them. For compounds **1**~**3**, ferromagnetic interactions exist between the Fe(Ⅲ) and Ni(Ⅱ) ions, which can be rationalized according to the orthogonality of the magnetic orbitals of the low-spin Fe(Ⅲ) and high-spin Ni(Ⅱ) ions[29-35]. Compared to compounds **2** and **3**, the Ni-N≡C bending angle of compound **1** is smaller, which presents a stronger ferromagnetic interaction. In addition, when the Ni-N≡C angles further decrease, an antiferromagnetic contribution will arise and the overall magnetic coupling would be weakened[35]. Although there exist $\pi\cdots\pi$ stacking interactions between the interchain in compound **1**, the nearest interchain Ni⋯Ni distance 1.454 8(6) nm is the largest among the three compounds. Such a large interchain distance will diminish the interchain magnetic interactions and benefit for the SCM behavior. It is worth noting that steric hindrance can enhance the bending of the C≡N-Ni angle and elongate the Ni-N bond lengths. The smaller bending angle of C≡N-Ni and shorter Ni-N bond length should be also responsible for the single-chain magnet behavior of compound **1**. For the ligand shape, these results indicate that the introduction of long monodentate ligand plays an important role for obtaining SCMs.

3　Conclusions

In summary, three new cyano-bridged $Fe^{Ⅲ}_2Ni^{Ⅱ}$ double-zigzag chains, $\{[Fe(bpy)(CN)_4]_2[Ni(bp)_2]\cdot2H_2O\}_n$ (**1**), $\{[Fe(bpy)(CN)_4]_2[Ni(papy)_2]\cdot H_2O\}_n$ (**2**) and $\{[Fe(bpy)(CN)_4]_2[Ni(azp)]\cdot4H_2O\}_n$ (**3**) were synthesized. The magnetic studies demonstrate the existence of ferromagnetic interactions between Fe(Ⅲ) and Ni(Ⅱ) ions and slow magnetic relaxation behavior of compound **1**. Compounds **2** and **3** show ferromagnetic behavior but no single-chain magnets property. Our results demonstrate that ancillary ligands play an important role in influencing the intra- and interchain interactions as well as the local coordination environments. This work is useful for the design of new SCMs in the future.

References:

[1] Myers E B, Ralph D C, Katine J A, et al. *Science*, **1999**, **285**:867-870

[2] Troiani F, Affronte M. *Chem. Soc. Rev.*, **2011**,**40**:3119-3129

[3] Shiraishi M, Ikoma T. *Chem. Soc. Rev.*, **2011**,**189**:95-127
[4] Rinehart J D, Long J R. *Chem. Sci.*, **2011**,**2**:2078-2085
[5] Cucinotta G, Perfetti M, Luzon J, et al. *Angew. Chem. Int. Ed.*, **2012**,**51**:1606-1610
[6] Wang C F, Zuo J L, Bartlett B M, et al. *J. Am. Chem. Soc.*, **2006**,**128**:7162-7163
[7] Guo Y N, Xu G F, Guo Y, et al. *Dalton Trans.*, **2011**,**40**:9953-9963
[8] Koo B H, Lim K S, Ryu D W, et al. *Chem. Commun.*, **2012**, **48**:2519-2521
[9] Glauber R J. *J. Math. Phys.*, **1963**,**4**:294-307
[10]Caneschi A, Gatteschi D, Lalioti N, et al. *Angew. Chem. Int. Ed.*, **2001**,**40**:1760-1763
[11]Clérac R, Miyasaka H, Yamashita M, et al. *J. Am. Chem. Soc.*, **2002**,**124**:12837-12844
[12]Palii A V, Reu O S, Ostrovsky S M, et al. *J. Am. Chem. Soc.*, **2008**,**130**:14729-14738
[13]Bogani L, Vindigni A. *J. Mater. Chem.*, **2008**,**18**:4750-4758
[14]Zhang W X, Ishikawa R, Breedlove B, et al. *RSC Adv.*, **2013**,**3**:3772-3798
[15]Liu T, Zheng H, Kang S, et al. *Nat. Commun.*, **2013**,**4**:2826-2832
[16]Heintze E, Hallak F E, Clauß C, et al. *Nat. Mater.*, **2013**,**12**:202-206
[17]ZHENG Hui(郑慧), XU Yang(徐杨), DUAN Chun-Ying(段春迎). *Chinese J. Inorg. Chem.*(无机化学学报), **2015**,**31**:1460-1466
[18]JIAO Cheng-Qi(矫成奇), JIANG Wen-Jing(姜文静), WEN Wen(文雯), et al. *Chinese J. Inorg. Chem.*(无机化学学报), **2016**,**32**:1637-1646
[19]Wang S, Ding X H, Li Y H, et al. *Coord. Chem. Rev.*, **2012**, **255**:1713-1732
[20]Zhang Y J, Liu T, Kanegawa S, et al. *J. Am. Chem. Soc.*, **2010**,**132**:912-913
[21]Jiang W, Jiao C, Meng Y, et al. *Chem. Sci.*, **2017**,**9**:617-622
[22]Miyasaka H, Julve M, Yamashita M, et al. *Inorg. Chem.*, **2009**,**48**:3420-3437
[23]Harris T D, Bennett M V, Clérac R, et al. *ChemInform*, **2010**,**41**:3980-3988
[24]Bernot K, Bogani L, Caneschi A, et al. *J. Am. Chem. Soc.*, **2006**,**128**:7947-7956
[25]Li X B, Zhang J Y, Wang Y Q, et al. *Chem. Eur. J.*, **2011**,**17**:13883-13891
[26]Luminita M T, Rodrigue L Z, Jorge P, et al. *J. Am. Chem. Soc.*, **2006**,**128**:4842-4853
[27]*SMART, SAINT* and *XPREP, Area Detector and Data Integration and Reduction Software*, Bruker Analytical Instruments Inc., Madison, WI, **1995**.
[28]Sheldtrick G M. *SHELXS*-97, *Program for X-ray Crystal Structure Solution and Refinement*, University of Göttingen, Germany, **1997**.
[29]Panja A, Guionneau P, Jeon I R, et al. *Inorg. Chem.*, **2012**, **51**:12350-12359
[30]Zhang Y Z, Mallik U P, Clérac R, et al. *Polyhedron*, **2013**, **52**:115-121
[31]Gu Z G, Yang Q F, Liu W, et al. *Inorg. Chem.*, **2006**,**45**:8895-8901
[32]Hoshino N, Sekine Y, Nihei M, et al. *Chem. Commun.*, **2010**,**46**:6117-6119
[33]Wang S, Zuo J L, Zhou H C, et al. *Inorg. Chim. Acta*, **2005**, **358**:2101-2106
[34]Wu D, Zhang Y, Huang W, et al. *Dalton Trans.*, **2010**,**39**:5500-5503
[35]Rebilly J N, Mallah T. *Struct. Bond.*, **2006**,**122**:103-131